Electrostatic influence of active-site waters on the nucleophilic aromatic substitution catalyzed by 4-chlorobenzoyl-CoA dehalogenase

Dingguo Xu, Hua Guo*

Department of Chemistry, University of New Mexico, Albuquerque, NM 87131, USA

Received 8 February 2005; revised 14 April 2005; accepted 28 June 2005

Available online 18 July 2005

Edited by Christian Griesinger

Abstract The 4-chlorobenzoyl-CoA dehalogenase catalyzes the hydrolytic dechlorination of 4-chlorobenzoyl-CoA via a two-step mechanism, namely nucleophilic aromatic substitution and ester hydrolysis. The mutation of an active-site Histidine residue has been shown to reduce the catalytic activity in both the substitution and subsequent hydrolysis steps. In this communication, we report a quantum mechanical/molecular mechanical simulation of the potential of mean force for the substitution step, which confirms the increased barrier height in the H90Q mutant and provides evidence on the electrostatic influence of two active-site waters on the rate-limiting barrier.

Keywords: Dehalogenase; QM/MM study; Electrostatic interactions

1. Introduction

The 4-chlorobenzoyl-CoA (4-CBA-CoA) dehalogenase is a unique enzyme found in soil-dwelling bacteria, which catalyzes the hydrolytic dechlorination of 4-CBA-CoA [1,2]. It has been identified as a key bioremediation catalyst for the removal of toxic chlorinated aromatics such as polychlorinated biphenyls (PCB) [3,4]. Apart from keen interests in designing novel and more efficient bioremediation catalysts, this enzyme also offers an ideal prototype to identify key factors that can affect the catalytic efficiency in this multitasking enzyme. As shown in Scheme 1, the proposed mechanism [5–9] involves the initial nucleophilic attack of the benzoyl C_4 of the enzyme–substrate (ES) complex by the carboxylate group of Asp145. This so-called nucleophilic aromatic substitution (S_NAr) step is believed to be via an enzyme-Meisenheimer (EMc) intermediate, featuring a covalently bounded anionic σ-complex [10]. The collapse of the EMc complex by expelling the chloride ion leads to the arylated enzyme (EAr) complex. In the second hydrolysis step, the EAr intermediate is attacked by a H_2O molecule activated by an active-site Histidine (H90) to form the 4-hydroxybenzoyl-CoA (4-HBA-CoA) product, whose release completes the catalytic cycle.

It is well established that electrostatic interactions play an important role in enzyme catalysis [11–13]. Unlike in aqueous solutions, the electrostatic environment in the enzyme active site is preorganized to lower the transition state energy, a phenomenon called "solvent substitution" [14]. In 4-CBA-CoA dehalogenase, for example, there is strong experimental [15–19] and theoretical evidence [20–22] that two backbone NH groups at the 64 and 114 positions, and possibly the α-helix terminated at Gly114, provide pre-organized electrostatic forces in the enzyme active site to stabilize the rate-limiting transition state in the S_NAr step as well as the EMc intermediate. On the other hand, the benzoyl moiety is surrounded by hydrophobic side chains of Phe82, Trp137, and Trp89. The electrophilic catalysis is partially responsible for the lowering of the barrier height from ~37 kcal/mol in aqueous solution [23] to about 17 kcal/mol in the enzyme [21,22].

As a continuation of our recent work [21,22], we report here a theoretical study of a key mutant of 4-CBA-CoA dehalogenase. Experimental work in the Dunaway-Mariano group has recently shown that the mutation of His90 to Gln reduced the hydrolysis rate by 154-fold [24]. This is consistent with the mechanism depicted in Scheme 1, in which His90 serves as the general base in activating the water nucleophile in the hydrolysis step. The small change in the rate can be understood in light of the good phenoxide leaving group. However, it was a surprise that the H90Q mutant also slowed down the substitution step by 133-fold. The X-ray structure of the enzyme-product (EP) complex of the mutant [24], shown in Fig. 1, indicates some rearrangement of the active site and the presence of two water molecules. Based on the structural and kinetic evidence, it was speculated that hydration of the active site might be responsible for the reduced catalytic activity for the S_NAr step. In this work, we investigate theoretically the free energy profile for the S_NAr reaction catalyzed by the 4-CBA-CoA mutant, and address the origin of the reduced catalytic activity.

It is perhaps worthwhile at this conjuncture to point out that the catalytic activity in the H90Q mutant may also be influenced by the side chain conformation of the 90th residue. As shown in Fig. 1, the Gln side chain in the H90Q mutant is pointing towards the solvent, while the imidazole of His in the wild-type (WT) enzyme forms a solvent barrier. It has been established from X-ray structures of the WT and mutant dehalogenases [9,24] and from molecular dynamics (MD) simulations [22] that conformational changes of the H90 side chain are possible and might be related to a kinetic step observed in multiple turnovers and to the release of the Cl^- product to the solvent. It follows that the Gln side chain in the H90Q mutant may also assume multiple conformational geometries. However, there is no concrete structural evidence supporting the conformational flexibility of the Q90 side chain. Because of the lack of experimental information, the effect of conformational changes in the H90Q mutant is not addressed in this work.

*Corresponding author. Fax: +1 505 277 2609.
E-mail address: hguo@unm.edu (H. Guo).

0014-5793/$30.00
doi:10.1016/j.febslet.2005.06.056

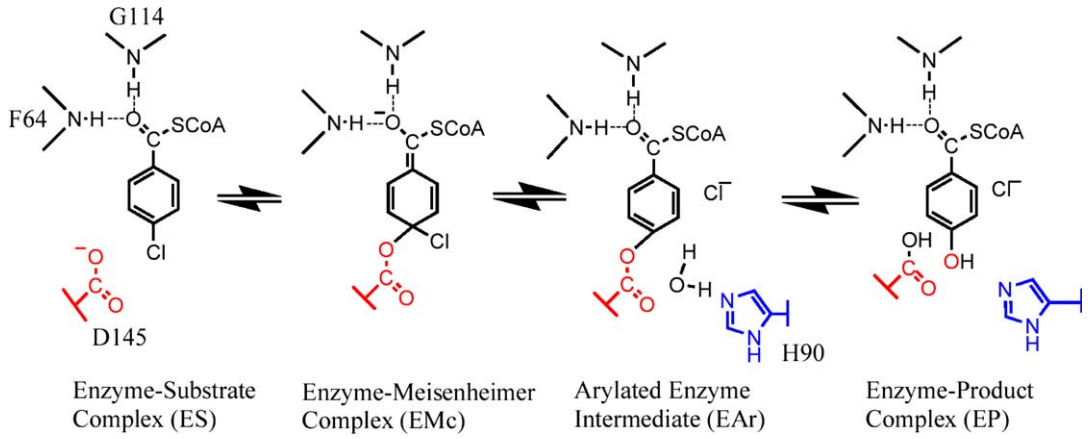

Scheme 1. Proposed kinetic model for the hydrolytic dechlorination of 4-CBA-CoA by 4-CBA-CoA dehalogenase.

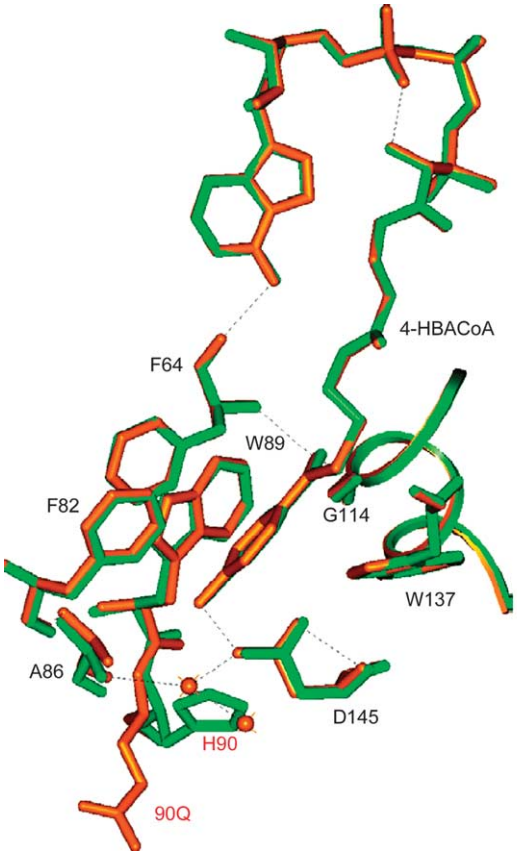

Fig. 1. Overlay of some key active site residues in the WT (green) and H90Q (orange) mutant of 4-CBA-CoA dehalogenase.

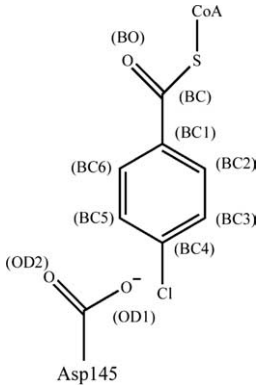

Scheme 2. Definition of atoms.

2. Methods

Because the computational methods used here have been extensively discussed in our earlier publication [22], only a brief outline is given. All calculations were performed using the Charmm suite of molecular simulation codes [25]. The initial coordinates of the system was adopted from the EP complex of the H90Q mutant (PDB code 1JXZ) [24] by replacing the hydroxyl oxygen of the 4-HBA group with chlorine. The resulting ES complex was then solvated in a 25 Å radius pre-equilibrated sphere of TIP3P waters [26] centered at Cl. Stochastic boundary conditions [27] were imposed, where the solvated ES complex is divided into three zones. The inner reaction zone ($r < 22$ Å) is governed by Newtonian dynamics, while the buffer zone ($22 < r < 25$ Å) is subjected to harmonic restraining potentials and Langevin dynamics. The atoms in the outer reservoir region were deleted. To account for long-range solvent screening effects, a simple charge scaling scheme [28] was used. The MD simulations employed the SHAKE algorithm [29] and a time step of 1 fs.

The potentials of mean force (PMFs) for the S_NAr reaction were simulated by umbrella sampling [30] and the weighted histogram analysis method (WHAM) [31]. The reaction coordinate is conveniently defined as $R_\phi = R_{BC4-Cl} - R_{OD1-BC4}$ and the atom labels are defined in Scheme 2. To efficiently compute the potential energy surface of this reactive system, we employed the quantum mechanical/molecular mechanical (QM/MM) approach [32–35], which partitions the system into the QM and classical MM regions. The QM region, which includes in the present work the carboxylate group of Asp145 and the benzoyl group of the substrate, was treated with the semi-empirical PM3 method [36]. The choice of the PM3 method was motivated by a recent theoretical study of a gas phase S_NAr reaction [23], which showed that the PM3 method yielded similar energies and geometries with the B3LYP/6-311 + G** level of theory. The semiempirical method may not be quantitatively accurate, but should be sufficient for comparing the same reaction in different microenvironments. Finally, the boundary atoms between the QM and MM regions, namely the C_α of Asp145 and C_β of the mercaptoethylamine part of CoA, was treated with the generalized hybrid orbital (GHO) approach [35].

3. Results and discussion

The reaction path along the putative reaction coordinate was first determined by adiabatic mapping, in which the energy

was minimized at pre-specified values of R_ϕ. These geometries were then used as the initial conditions in the PMF calculations. Twenty-five separate windows were employed along the reaction coordinate with a harmonic biasing potential in each window. The force constant of the umbrella potential ranges from 70 to 100 kcal/mol Å^2. For each window, the system is allowed to equilibrate for 50 ps before the 50 ps data collection.

The PMF for the S_NAr reaction catalyzed by the H90Q mutant of 4-CBA-CoA dehalogenase is displayed in Fig. 2. For comparison, the PMF for the WT dehalogenase is also included in the figure. The overall shapes of the free energy profiles are quite similar, featuring the EMc intermediate flanked by the rate-limiting addition barrier and a much lower elimination barrier. An important difference is that the addition barrier of the mutant is about 1.8 kcal/mol higher than that of the WT enzyme. The increase in this rate-limiting barrier is in good, but not perfect, agreement with the experimentally observed 133-fold reduction of catalytic rate in the H90Q mutant, which corresponds to a 2.9 kcal/mol increase in barrier height. Interestingly, the energy of the EMc intermediate is also increased by 5.2 kcal/mol in the mutant.

A careful analysis of the charge distribution and bond lengths along the reaction path indicates that the catalytic mechanism of the S_NAr reaction is not substantially altered by the mutation. Fig. 3 displays the Mulliken charges of some key atoms and selected bond lengths, which are qualitatively similar to those obtained from the S_NAr reaction catalyzed by the WT enzyme [22]. Like in the WT enzyme, significant charge migration takes place within the benzoyl moiety upon the nucleophilic attack of the Asp145 carboxylate. Near the rate-limiting transition state, for example, there is notable negative charge buildup at the carbonyl carbon of the benzoyl group, which is five bonds away from C_4. In addition, the benzoyl carbonyl bond is elongated, reflecting the increased single bond characteristics. The corresponding benzene ring becomes distorted to a quinone-like structure with alternating single and double bonds. Throughout the reaction, on the other hand, the hydrogen bonds between the benzoyl carbonyl oxygen and the backbone NH groups of Phe64 and Gly114 are always maintained. In fact, the hydrogen bond interactions increase near $R_\phi \sim 0$, presumably due to the negative charge buildup at the benzoyl carbonyl. In particular, the CO···HN distances for the hydrogen bonds to Gly114 and Phe64 change from 1.96 and 2.17 Å in the reactant complex to 1.90 and 2.02 Å at the rate-limiting transition state.

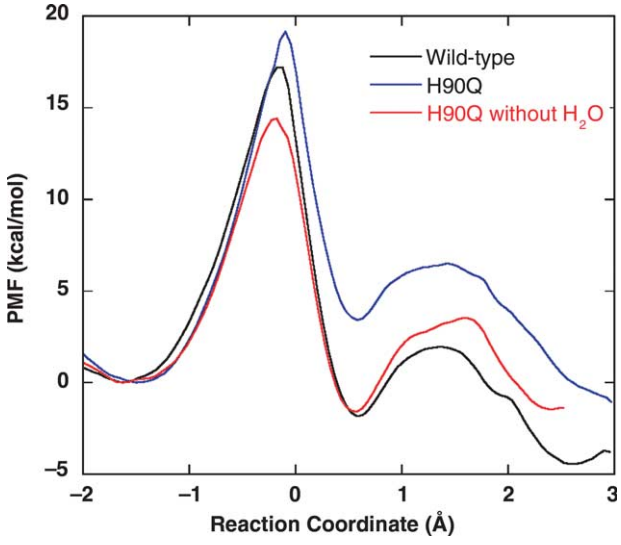

Fig. 2. Calculated PMFs for the S_NAr reaction catalyzed by the WT enzyme (black), the H90Q mutant (blue), and H90Q mutant without active site water (red).

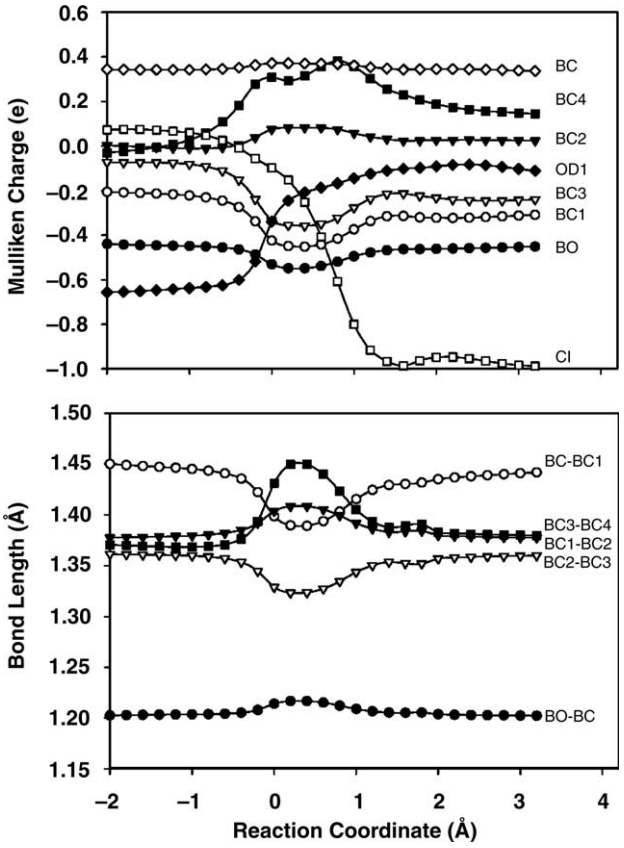

Fig. 3. Mulliken charges of some key atoms (upper panel) and selected bond lengths along the reaction path.

To elucidate the origin of the increased barrier, we repeated the PMF calculation without the active-site water molecules (W274 and W549). The resulting PMF, which is also shown in Fig. 2, indicates a much lower barrier. In fact, the reduction of 4.6 kcal/mol makes the rate-limiting barrier even lower than that for the WT enzyme. Although many other factors may also contribute, these results strongly suggest an important role played by the active site water molecules in the mutant, which are absent in the active site of the WT enzyme [9]. The negative impact of the active site water on the catalytic efficiency of the enzyme is not difficult to understand. It is well established [23] that solvation in polar solvents can significantly increase the barrier for the S_NAr reaction, due largely to the relative stabilization of the reactant. As shown in Fig. 1, the two water molecules are in contact with the nucleophile.

To further elucidate the role played by the active-site water molecules, we have carried out a charge perturbation analysis [37] along the reaction path, which sheds light on their electrostatic contributions to the stabilization of the rate-limiting transition state. The basic idea is to determine the energy

difference when the atomic charges of the two water molecules are scaled to zero. In particular, the energy difference is defined as follows:

$$\Delta\Delta E = \Delta E_{TS} - \Delta E_{ES}$$

with $\Delta E = E^{scale} - E^{non\text{-}scale}$. Hence, a negative $\Delta\Delta E$ corresponds to stabilization of the transition state relative to the reactant when the charges are zeroed. For W549 and W274, the zeroing of their charges results in $\Delta\Delta E = -2.3$ and -1.5 kcal/mol, respectively. The combined destabilization energy of 3.8 kcal/mol for the transition state is consistent with the 4.6 kcal/mol reduction in barrier height observed in the PMF when the active-site waters were taken out (Fig. 2). The residual energy change can presumably be attributed to the rearrangement of the protein. This result clearly identified the electrostatic origin of the interaction and provides strong support to the hypothesis [24] that the hydration of the active site is responsible for the reduced catalytic efficiency in the H90Q mutant.

4. Conclusions

In this work, we employed a QM/MM method to elucidate the reduced efficiency of the H90Q mutant of 4-CBA-CoA dehalogenase in catalyzing the S_NAr reaction. The calculated mutant PMF confirmed the increased barrier height for the rate-limiting nucleophilic addition step when compared with the WT enzyme, although the catalytic mechanism was found to be unchanged. The increased barrier is attributed to the presence of water molecules in the active site, which provide partial solvation of the nucleophile. The electrostatic origin of the interaction was identified by a charge perturbation analysis.

An important caveat about the above conclusion is that the influence of conformational flexibility of the Q90 side chain is not considered in our model. Such conformational changes are expected to be very slow and thus difficult to simulate. However, they may be related to a discrete and sometimes rate-limiting kinetic step observed in the experiment and may be responsible for the release of the Cl^- product formed in the substitution step. The influence of side chain conformational changes in the 90th position is thus an important and challenging problem to be resolved by future simulations.

The 4-CBA-CoA dehalogenase catalyzes two very different reactions. The first S_NAr reaction favors a hydrophobic environment, because solvation in polar solvent selectively stabilizes the reactant [23]. Indeed, the benzoyl moiety is surrounded by aromatic rings of several active-site residues. On the other hand, the second general base-catalyzed ester hydrolysis prefers a polar surrounding, which lowers the energy of the zwitterionic transition state [38]. The enzyme thus has to compromise and provide perfect electrostatic to neither steps. Indeed, the evolution of this enzyme, judging from its k_{cat}/K_m of $1.6 \times 10^5\ s^{-1}\ M^{-1}$ [18], is still far from perfection. The results presented in this work highlight the dilemma faced by such an enzyme: a reduced hydrophilicity at the active site will accelerate the first S_NAr step, but at the price of slowing down the second hydrolysis step, and vice versa. This feature of this multitasking enzyme poses a challenge for designing novel and more efficient bioremediation catalysts.

Acknowledgements: This work was supported by the National Science Foundation. We thank Prof. D. Dunaway-Mariano and Dr. Yansheng Wei for providing Fig. 1 and many insightful discussions.

References

[1] Scholten, J.D., Chang, K.-H., Babbitt, P.C., Charest, H., Sylvestre, M. and Dunaway-Mariano, D. (1991) Novel enzymic hydrolytic dehalogenation of a chlorinated aromatic. Science 253, 182–185.
[2] Dunaway-Mariano, D. and Babbitt, P.C. (1994) On the origins and functions of the enzymes of the 4-chlorobenzoate to 4-hydroxybenzoate converting pathway. Biodegradation 5, 259–276.
[3] Abramowicz, D.A. (1990) Aerobic and anaerobic biodegradation of PCBs: a review. Crit. Rev. Biotechnol. 10, 241–248.
[4] Commandeur, L.C.M. and Parsons, J.R. (1990) Degradation of halogenated aromatic compounds. Biodegradation 1, 207–220.
[5] Yang, G., Liang, P.-H. and Dunaway-Mariano, D. (1994) Evidence for nucleophilic catalysis in the aromatic substitution reaction catalyzed by (4-chlorobenzoyl) coenzyme A dehalogenase. Biochem 33, 8527–8531.
[6] Liu, R.-Q., Liang, P.-H., Scholten, J. and Dunaway-Mariano, D. (1995) Transient state kinetic analysis of the chemical intermediates formed in the enzymatic dehalogenation of 4-chlorobenzoyl coenzyme A. J. Am. Chem. Soc. 117, 5003–5004.
[7] Yang, G., Liu, R., Taylor, K.L., Xiang, H., Price, J. and Dunaway-Mariano, D. (1996) Identification of active site residues essential to 4-chlorobenzoyl-coenzyme A dehalogenase catalysis by chemical modification and site directed mutagenesis. Biochem 35, 10879–10885.
[8] Crooks, G.P., Xu, L., Barkley, R.M. and Copley, S.D. (1995) Exploration of possible mechanisms for 4-chlorobenzoyl CoA dehalogenase: evidence for an aryl-enzyme intermediate. J. Am. Chem. Soc. 117, 10791–10798.
[9] Benning, M.M., Taylor, K.L., Liu, R.-Q., Yang, G., Xiang, H., Wesenberg, G., Dunaway-Mariano, D. and Holden, H.M. (1996) Structure of 4-chlorobenzoyl coenzyme A dehalogenase determined to 1.8 Å resolution: an enzyme catalyst generated via adaptive mutation. Biochem 35, 8103–8109.
[10] Miller, J. (1968)Aromatic Nucleophilic Substitution, Elsevier, Amsterdam.
[11] Jencks, W.P. (1986)Catalysis in Chemistry and Enzymology, Dover, New York.
[12] Warshel, A. (1978) Energetics of enzyme catalysis. Proc. Natl. Acad. Sci. USA 75, 5250–5254.
[13] Warshel, A. (1998) Electrostatic origin of the catalytic power of enzymes and the role of preorganized active sites. J. Biol. Chem. 273, 27035–27038.
[14] Warshel, A., Aqvist, J. and Creighton, S. (1989) Enzymes work by solvation substitution rather than by desolvation. Proc. Natl. Acad. Sci. USA 86, 5820–5824.
[15] Taylor, K.L., Liu, R.-Q., Liang, P.-H., Price, J. and Dunaway-Mariano, D. (1995) Evidence for electrophilic catalysis in the 4-chlorobenzoyl-CoA dehalogenase reaction: UV, Raman, and 13C-NMR spectral studies of dehalogenase complexes of benzoyl-CoA adducts. Biochem 34, 13881–13888.
[16] Taylor, K.L., Xiang, H., Liu, R.-Q., Yang, G. and Dunaway-Mariano, D. (1997) Investigation of substrate activation by 4-chlorobenzoyl-coenzyme A dehalogenase. Biochem 36, 1349–1361.
[17] Dong, J., Xiang, H., Luo, L., Dunaway-Mariano, D. and Carey, P.R. (1999) Modulating electron density in the bound product, 4-hydroxybenzoyl-CoA, by mutations in 4-chlorobenzoyl-CoA dehalogenase near the 4-hydroxy group. Biochem 38, 4198–4206.
[18] Luo, L., Taylor, K.L., Xiang, H., Wei, Y., Zhang, W. and Dunaway-Mariano, D. (2001) Role of active site binding interactions in 4-chlorobenzoyl-coenzyme A dehalogenase catalysis. Biochem 40, 15684–15692.
[19] Dong, J., Lu, X., Wei, Y., Luo, L., Dunaway-Mariano, D. and Carey, P.R. (2003) The strength of dehalogenase-substrate hydrogen bonding correlates with the rate of Meisenheimer intermediate formation. Biochem 42, 9482–9490.

[20] Lau, E.Y. and Bruice, T.C. (2001) The active site dynamics of 4-chlorobenzoyl-CoA dehalogenase. Proc. Natl. Acad. Sci. USA 98, 9527–9532.
[21] Xu, D., Guo, H., Gao, J. and Cui, Q. (2004) A QM/MM study of a nucleophilic aromatic substitution reaction catalyzed by 4-chlorobenzoyl-CoA dehalogenase. Chem. Commun., 892–893.
[22] Xu, D., Wei, Y., Wu, J., Dunaway-Mariano, D., Guo, H., Cui, Q. and Gao, J. (2004) QM/MM studies of enzyme catalyzed dechlorination reaction of 4-chlorobenzoyl-CoA provide insight into reaction energetics. J. Am. Chem. Soc. 126, 13649–13658.
[23] Zheng, Y.-J. and Bruice, T.C. (1997) On the dehalogenation mechanism of 4-chlorobenzoyl CoA by 4-chlorobenzoyl CoA dehalogenase: insights from study based on the nonenzymatic reaction. J. Am. Chem. Soc. 119, 3868–3877.
[24] Zhang, W., Wei, Y., Luo, L., Taylor, K.L., Yang, G., Dunaway-Mariano, D., Benning, M.M. and Holden, H.M. (2001) Histidine 90 function in 4-chlorobenzoyl-coenzyme A dehalogenase catalysis. Biochem 40, 13474–13482.
[25] Brooks, B.R., Bruccoleri, R.E., Olafson, B.D., States, D.J., Swaminathan, S. and Karplus, M. (1983) Charmm: a program for macromolecular energy, minimization, and dynamics calculations. J. Comput. Chem. 4, 187–217.
[26] Jorgensen, W.L., Chandrasekhar, J., Madura, J.D., Impey, R.W. and Klein, M.L. (1983) Comparison of simple potential functions for simulating liquid water. J. Chem. Phys. 79, 926–935.
[27] Brooks III, C.L. and Karplus, M. (1989) Solvent effects on protein motion and protein effects on solvent motion. J. Mol. Biol. 208, 159–181.
[28] Simonson, T., Archontis, G. and Karplus, M. (1997) Continuum treatment of long-range interactions in free energy calculations. Application to protein–ligand binding. J. Phys. Chem. B 101, 8349–8362.
[29] Ryckaert, J.P., Ciccotti, G. and Berendsen, H.J. (1977) Numerical integration of the cartesian equations of motion of a system with constraints: molecular dynamics of *n*-alkanes. J. Comput. Phys. 23, 327–341.
[30] Torrie, G.M. and Valleau, J.P. (1977) Non-physical sampling distributions in Monte Carlo free energy estimation: umbrella sampling. J. Comput. Phys. 23, 187–199.
[31] Kumar, S., Bouzida, D., Swendsen, R.H., Kollman, P.A. and Rosenberg, J.M. (1992) The weighted histogram analysis method for free energy calculations on biomolecules. 1. The method. J. Comput. Chem. 13, 1011–1021.
[32] Warshel, A. and Levitt, M. (1976) Theoretical studies of enzymatic reactions: dielectric, electrostatic and steric stabilization of carbonium ion in the reaction of lysozyme. J. Mol. Biol. 103, 227–249.
[33] Singh, U.C. and Kollman, P.A. (1986) A combined ab initio quantum mechanical and molecular mechanical method for carrying out simulations on complex molecular systems: applications to the $CH_3Cl + Cl^-$ exchange reaction and gas-phase protonation of polyethers. J. Comput. Chem. 7, 718.
[34] Field, M.J., Bash, P.A. and Karplus, M. (1990) A combined quantum mechanical and molecular mechanical potential for molecular dynamics simulations. J. Comput. Chem. 11, 700–733.
[35] Gao, J., Amara, P., Alhambra, C. and Field, M.J. (1998) A generalized hybrid orbital (GHO) method for the treatment of boundary atoms in combined QM/MM calculations. J. Phys. Chem. A 102, 4714–4721.
[36] Stewart, J.J.P. (1989) Optimization of parameters for semi-empirical methods. 1. Method. J. Comput. Chem. 10, 209–220.
[37] Bash, P.A., Field, M.J., Davenport, R.C., Petsko, G.A., Ringe, D. and Karplus, M. (1991) Computer simulation and analysis of the reaction pathway of triosephosphate isomerase. Biochem 30, 5826–5832.
[38] Xie, D., Xu, D., Zhang, L. and Guo, H. (2005) Theoretical study of general base-catalyzed hydrolysis of aryl esters and implications for enzymatic reaction. J. Phys. Chem. B 109, 5259.